Quantitative high-throughput screening: A titration-based approach that efficiently identifies biological activities in large chemical libraries

James Inglese*, Douglas S. Auld, Ajit Jadhav, Ronald L. Johnson, Anton Simeonov, Adam Yasgar, Wei Zheng, and Christopher P. Austin

NIH Chemical Genomics Center, National Human Genome Research Institute, National Institutes of Health, Bethesda, MD 20892-3370

Communicated by Francis S. Collins, National Institutes of Health, Bethesda, MD, May 31, 2006 (received for review April 12, 2006)

High-throughput screening (HTS) of chemical compounds to identify modulators of molecular targets is a mainstay of pharmaceutical development. Increasingly, HTS is being used to identify chemical probes of gene, pathway, and cell functions, with the ultimate goal of comprehensively delineating relationships between chemical structures and biological activities. Achieving this goal will require methodologies that efficiently generate pharmacological data from the primary screen and reliably profile the range of biological activities associated with large chemical libraries. Traditional HTS, which tests compounds at a single concentration, is not suited to this task, because HTS is burdened by frequent false positives and false negatives and requires extensive follow-up testing. We have developed a paradigm, quantitative HTS (qHTS), tested with the enzyme pyruvate kinase, to generate concentration–response curves for >60,000 compounds in a single experiment. We show that this method is precise, refractory to variations in sample preparation, and identifies compounds with a wide range of activities. Concentration–response curves were classified to rapidly identify pyruvate kinase activators and inhibitors with a variety of potencies and efficacies and elucidate structure–activity relationships directly from the primary screen. Comparison of qHTS with traditional single-concentration HTS revealed a high prevalence of false negatives in the single-point screen. This study demonstrates the feasibility of qHTS for accurately profiling every compound in large chemical libraries (>10^5 compounds). qHTS produces rich data sets that can be immediately mined for reliable biological activities, thereby providing a platform for chemical genomics and accelerating the identification of leads for drug discovery.

1,536-well | chemical genomics | enzyme assay | PubChem | pyruvate kinase

The first description of biological effect versus chemical compound concentration was made by Paracelsus *ca*. 1534 and quantified by A. V. Hill in 1910 (1). The basis of these observations is that ligands affecting biological systems have optimal ranges of activity (EC_{50}), and give rise to concentration–effect relationships that can be complex, varying in potency, efficacy, and steepness of response. Far below an EC_{50}, no effect may be seen (referred to as the no observable effect level or NOEL), and much above it, toxic or "off-target" effects may be observed. This well known behavior of chemical compounds in biological systems requires a specific dose of a compound to achieve a desired biological effect, whether in basic or clinical applications (2, 3).

Historically, new compounds with medicinal qualities were discovered through laborious testing of samples using low-throughput assays including animal and isolated tissue models. In the early 1990s, the advent of combinatorial chemistry and commercial consolidation of small molecule collections resulted in a tremendous increase in compound numbers, requiring the development of high-throughput screening (HTS) (4). In addition, sensitive *in vitro* assays became readily available with the advancement of techniques to produce recombinant proteins and engineered cell lines. Screening large chemical libraries was sufficiently technically demanding that the methodology focused on assaying a single concentration of each compound. Although this technology enabled the screening of collections exceeding one million small molecules, it has been burdened by high numbers of false positives and putative false negatives (5) as well as the inability to identify subtle complex pharmacology, such as partial agonism or antagonism.

To address these limitations of traditional HTS, we used advanced screening technologies, such as low-volume dispensing, high-sensitivity detectors, and robotic plate handling, to develop a titration-based screening approach. To demonstrate this process, we used an enzymatic assay designed to detect both activators and inhibitors in a homogenous format. A procedure was developed to plate compounds at seven or more concentrations in 1,536-well plate format to screen the assay against >60,000 compounds in compound-titration series. Rapid fitting and classification of the concentration–response curves were developed to enhance and weigh appropriately the structure–activity relationship (SAR) revealed from the screen. By using this quantitative HTS (qHTS) methodology, enzyme modulators with a variety of pharmacologies were detected and clear SAR delineated directly from the primary screen.

These results demonstrate the ability of qHTS to rapidly identify new *in vitro* chemical probes and produce comprehensive library-bioactivity information suitable for initiation of medicinal chemistry for both *in vivo* chemical probes and drug development (6). By providing reliable measures of compound behavior across biological processes, qHTS generates data sets that can be compared to identify compounds with narrow or wide spectra of bioactivity as well as activities not modulated by current libraries, thus guiding compound library expansion into novel chemical space. In so doing, qHTS provides a platform for building a high-quality publicly available (7) chemical genomic data set, with broad utility for deriving the general principles governing interactions of small molecules with their targets.

Results

Preparation of 1,536-Well Plate-Titration Plates. Quantitative HTS requires a chemical library prepared as a titration series. To establish a concentration–response series, we prepared at least seven 5-fold dilutions that resulted in a concentration range of approximately four orders of magnitude. To maximize flexibility,

Conflict of interest statement: No conflicts declared.

Freely available online through the PNAS open access option.

Abbreviations: AC_{50}, half-maximal activity concentration; HTS, high-throughput screening; qHTS, quantitative HTS; PK, pyruvate kinase; SAR, structure–activity relationship.

Data deposition: The bioassays reported in this paper have been deposited in the PubChem database, http://pubchem.ncbi.nlm.nih.gov (ID codes 361, 410, and 411).

*To whom correspondence should be addressed at: NIH Chemical Genomics Center, National Human Genome Research Institute, National Institutes of Health, 9800 Medical Center Drive, Bethesda, MD 20892-3370. E-mail: jinglese@mail.nih.gov.

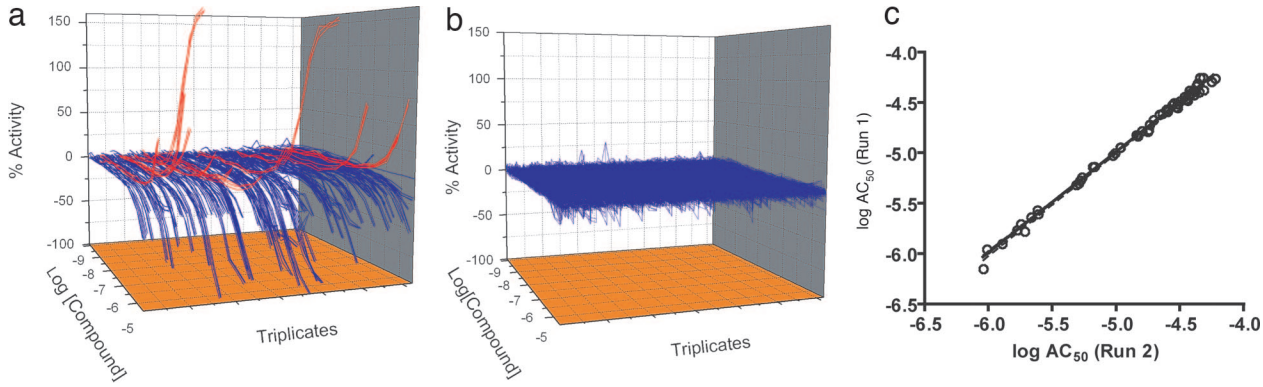

Fig. 1. Reproducibility of PK qHTS. Interscreen data from triplicate qHTS runs of the Prestwick collection. (*a*) Data for 104 compounds fitting concentration–response curves with inhibitory (blue) or stimulatory (red) activity are shown. Lines connect the data points for each compound titration and replicate. (*b*) Data for 1,016 compounds did not fit to a concentration–response curve. (*c*) Representative correlation plot of compounds with AC_{50} <60 μM identified from runs 1 and 2 (r^2 = 0.98; n = 58; median MSR = 1.1). For runs 1 vs. 3 and 2 vs. 3, r^2 = 0.99 and 0.98, respectively.

titrations were done between plates, producing a replicate of the entire library at seven different concentrations. For the majority of the compound collection, the resulting concentrations in the source plates ranged from 640 nM to 10 mM. After pin tool transfer into an assay volume of 4 μl, the final compound concentrations ranged from 3.7 nM to 57 μM.

Pyruvate Kinase (PK) qHTS. To test the qHTS paradigm, we assayed PK, a well characterized enzyme that is allosterically regulated (8, 9). PK regenerates ATP in glycolysis by catalyzing phosphoryl transfer from phosphoenol pyruvate to ADP to yield pyruvate and ATP. PK-mediated generation of ATP was assayed indirectly through the coupling to luciferase activity. Luciferase catalyzes the oxidation of luciferin in an ATP-dependent manner, yielding a luminescence signal. The assay was designed to detect both inhibitors and activators of PK activity. In addition, ribose-5-phosphate (R5P), a known allosteric activator of PK (8), and luteolin, a flavonoid that we identified as a PK inhibitor, were used as activator and inhibitor controls respectively.

We initially tested the reproducibility of the concentration–response curves by screening the Prestwick collection (1,120 samples) in triplicate. Curve fits were generated, and half-maximal activity concentration (AC_{50}) values were calculated for the 104 active compounds. Comparison of 58 actives with <60 μM AC_{50}, the highest tested concentration, from the three runs showed excellent agreement, suggesting that the liquid-handling and compound-transfer procedure was precise. Both weak and potent AC_{50} values were reproducible (Fig. 1*a*), and inactive compounds were consistently inactive in all replicate runs (Fig. 1*b*). Furthermore, a comparison of the AC_{50} values between each of the runs revealed a tight correlation, as measured by linear regression ($r^2 \geq 0.98$, Fig. 1*c*). Collectively, these results demonstrated that the qHTS methodology yielded highly accurate and precise data.

To test our process on a larger scale, we screened the PK assay against 60,793 compounds as concentration–response titrations (Fig. 2*a*). A total of 368 plates containing 565,248 wells were screened in automated format over a continuous 30-h period. The assay performed well over the entire course of the screen; control wells for each plate averaged a signal/background ratio of 9.6, and the Z' (10), a standard statistical measure of assay quality for single-concentration-based screening, averaged 0.87. The Z score of the experimental wells was 0.75 after correction for systematic artifacts. The concentration–response curves for the control activator R5P and the control inhibitor luteolin, included on every screening plate, were remarkably consistent, with median minimum significance ratio (MSR) (11) values of 1.7 and 1.2, respectively (Fig. 2*b*).

We examined the effect of sample preparation on qHTS reproducibility by evaluating concentration–response curves of 22 active compounds that were acquired independently from different suppliers. These duplicate samples were components of distinct libraries that were plated on separate occasions and resided in different plates. The AC_{50} correlation plot for these "intervendor duplicates" showed a lower correlation (r^2 = 0.81) compared with the interscreen replicates, with approximately half of the compounds having significantly different AC_{50} values (Fig. 2*c*). This result shows the degree of variability of independently acquired samples. Sample inconsistency, because of differences in compound preparation or

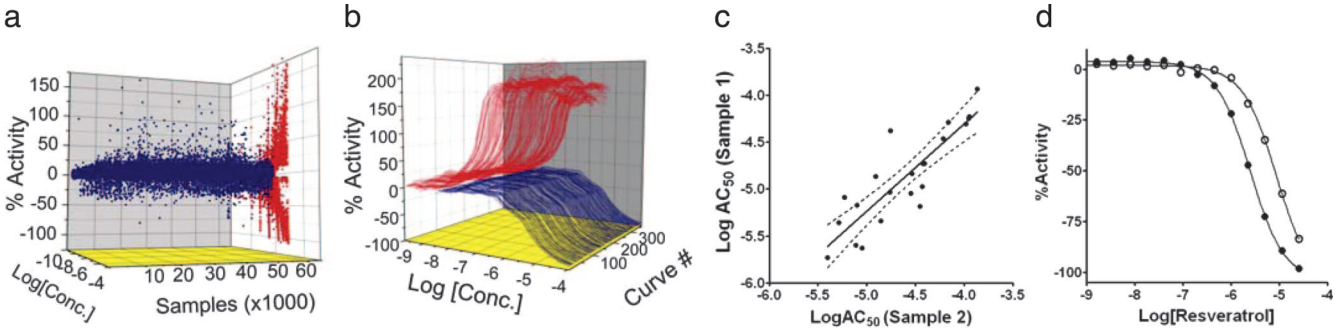

Fig. 2. qHTS of PK. (*a*) A 3D scatter plot of qHTS data lacking (blue) or showing (red) concentration–response relationships were obtained for all 60,793 samples. (*b*) All 368 intraplate titration curves for the control activator R5P (red) and the control inhibitor luteolin (blue) are shown. Lines connect the data for each titration. (*c*) Correlation plot of duplicate actives with AC_{50} <60 μM (r^2 = 0.81; n = 22; median MSR = 4). (*d*) Titration of independent resveratrol samples derived from the screen.

Table 1. Curve classification criteria

Curve class	Description	Efficacy	r^2	Asymptotes	Inflection
1*	Complete response (a)	>80% (a)	≥0.9 (a)	2	Yes
	Partial response (b)	≤80% (b)	≥0.9 (b)	2	Yes
2†	Incomplete curve	>80% (a) <80% (b)	>0.9 (a) <0.9 (b)	1	Yes
3	Single point activity	>Min‡	NA	1	No
4	Inactive	NA	NA	0	No

*AC_{50} derived from data.
†AC_{50} extrapolated from data.
‡Minimum (Min) is >3 SD from the mean activity of the sample field at the highest tested concentration.

stability, for example, is a particularly important consideration for traditional HTS, where actives are identified outside a defined threshold value. When this threshold is near the inflection point of the concentration–response curve, a small change in sample preparation could result in a compound no longer being classified as active, an important concern in traditional HTS (12). For example, resveratrol would be identified as active at 2.3 μM in one sample but inactive in the other, when a 50% threshold is used (Fig. 2*d*), despite having closely related concentration–response curves. By using qHTS, the entire concentration–response curve is obtained, and such potential false negatives are eliminated.

Concentration–Response Analysis. Automated analysis of qHTS data revealed a wide variety of concentration–response curves. To broadly define and encompass the diversity of these curves, we devised criteria to classify curves based on the quality of curve fit to the data (r^2), the magnitude of the response (efficacy), and the number of asymptotes to the calculated curve.

Based on this analysis, curves were organized into four categories, defined as follows (Table 1 and Fig. 3). Class 1a curves were well fit ($r^2 \geq 0.9$), showed a full response (efficacy >80%), and exhibited upper and lower asymptotes. Class 1b curves were the same as Class 1a except the efficacy value (30–80%) indicated a full but shallow curve. The 30% threshold for efficacy was derived from three SD above the mean activity of all samples at their highest tested concentration. Class 2 curves were incomplete; they contained only one asymptote and were divided into two subclasses. Class 2a had a good fit ($r^2 \geq 0.9$) and a sufficient response (efficacy >80%) to calculate an inflection point, whereas Class 2b characterized a weaker response (efficacy <80% and $r^2 < 0.9$). Class 3 curves displayed activity only at the highest tested concentration and efficacy >30%. Class 4 assignments were titrations with insufficient (efficacy <30%) or no response and are hereafter referred to as inactive (Fig 7, which is published as supporting information on the PNAS web site). Hence, the library in its entirety was defined as either active (Class 1–3) or inactive (Class 4).

By using these criteria, 5,480 of 60,793 compounds (9.0%) comprising Classes 1–3 were classified as active, whereas the remaining 91% were inactive (Fig. 4*a*). The identified actives consisted of 79% inhibitors and 21% activators and included the ATP competitive inhibitors apigenin and indirubin-3′-monoxime as well as the PK activator AMP (8), thus demonstrating the biological relevance of the screen. Of the active compounds, 9% (0.8% of the library) showed complete titration–response curves of full (4% Class 1a) or partial (5% Class 1b) activity, 30% were incomplete curves (8% and 22% Class 2a and -b, respectively), and 61% displayed activity mostly at the highest tested concentration (Class 3). Subdivision of actives into classes that reflect the curve-fit quality (r^2) of the concentration–response curves allowed us to consider pharmacological parameters in subsequent analysis.

The potency of the actives spanned three orders of magnitude, with AC_{50} values ranging from 55 nM to >100 μM. When actives were binned by potency, 4 compounds were <0.1 μM, 62 were from 0.1 to 1 μM, 595 were from 1 to 10 μM, and 4,819 were >10 μM. Class 1 curves spanned most of this range, from 55 nM to 51 μM, indicating that well fit, complete curves could be obtained from compounds of widely varying potency (Fig. 4*b*). Most of Class 2a curves had AC_{50} values between 1 and 10 μM, whereas the majority of Class 2b curves were >10 μM, consistent with their classification as incomplete curves. The AC_{50} values of Class 3 curves were extrapolated beyond the tested concentration range, indicating much lower potencies of uncertain accuracy. However, Class 3 curve fits were largely reproducible, as inferred from the triplicate Prestwick screen, where 74% of the 85 Class 3 actives were fit in all three runs, and an additional 16% fit in two of the three runs.

Interestingly, the Class 1b curves, those with lower efficacy, displayed a lower potency distribution compared with Class 1a. This observation suggests that compounds corresponding to Class 1b may have limited solubility and, therefore, decreased apparent potency. However, ALog P, a calculated property to estimate compound solubility, did not correlate with efficacy (Fig. 8, which is published as supporting information on the PNAS web site). Furthermore, this observation may be attributed to compounds selectively interacting with an enzyme subpopulation such as that seen in uncompetitive inhibition (13).

Comparison to Single-Concentration Screening Data Sets. To measure the frequency of false positives and false negatives observed in a traditional single-concentration screen, we undertook a retrospective analysis comparing the full concentration–response data set to the 11 μM titration point. When screening at one concentration, the probability of designating a certain compound as active

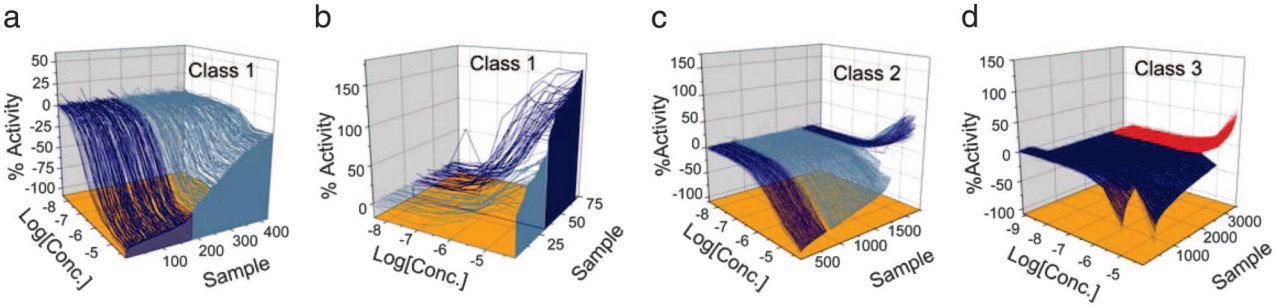

Fig. 3. Classes of titration curves obtained from the qHTS. Lines connecting titration data corresponding to inhibitory and stimulatory compounds are shown. (*a*) Classes 1a (blue) and 1b (teal) inhibitors display full and partial activity, respectively. (*b*) Classes 1a (blue) and 1b (teal) activators. (*c*) Incomplete curves for inhibitors and activators having AC_{50} values within and beyond the tested titration range are Classes 2a (blue) and 2b (teal), respectively. (*d*) Incomplete inhibitory (blue) and stimulatory (red) curves that show weak activity and poor fits are Class 3. Curve classes are defined further in Table 1.

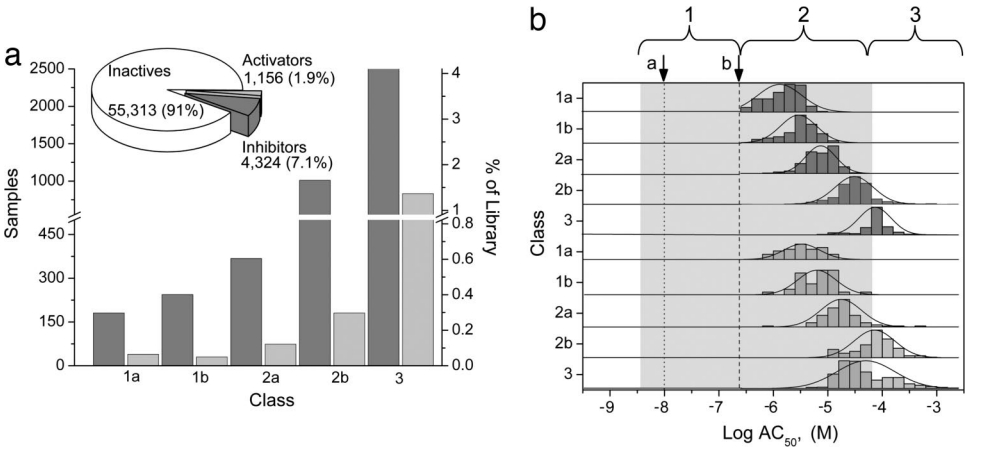

Fig. 4. Pharmacological profile of library activity. (*a*) Number and percentage of activators and inhibitors in each curve class. (*Inset*) Distribution of activators (light gray), inhibitors (dark gray), and inactives identified from the qHTS. (*b*) AC_{50} distribution of activators and inhibitors in each curve class. Regions 1, 2, and 3 indicate concentration ranges of absent, observed, and extrapolated potencies, respectively. The shaded area indicates the concentration range tested. Arrow a indicates the enzyme concentration (10 nM) at which the lowest AC_{50} can be observed, whereas arrow b is the no observable effect level (NOEL). To represent the range and average activity of a series, a normal distribution fit was calculated by using Origin software based on the maximum, minimum, and mean of the activity data.

is determined by the chosen screening concentration, the threshold value used to select the positives, and the potency of the compound (14). Determining where the threshold is set frequently depends on the library size, follow-up capacity (e.g., cherry-picking capacity, the nature of secondary assays), and the project-specific considerations (e.g., priority of target, desired potency). We applied two commonly applied thresholds, three and six SD from the mean activity of the screened compounds (≈30% and 60% of the 11 μM data set, respectively).

By using these limits, false positives and false negatives were enumerated for the 11 μM data set. False positives were compounds identified as active at the 11 μM concentration but classified as inactive (Class 4) by qHTS. False negatives were compounds identified as inactive at the 11 μM concentration but categorized as active (Class 1 or 2) by qHTS. Of the 5,480 actives identified by qHTS, only 1,461 were designated as active when a three-SD threshold was used. Twenty-seven percent corresponded to Class 1, 71% were Classes 2 and 3, and 2.0% comprised inactives and were therefore false positives (Fig. 5). At a more stringent threshold of six SD, 539 compounds were designated as active, of which 49% were Class 1, 50% were Classes 2 and 3, and 1.0% were inactive. Although a six-SD threshold increased the number of actives with Class 1 curves by 20% and decreased the number of false positives by half, 63% of the actives were eliminated. Hence, raising the threshold stringency decreased the number of positives and did little to recover additional Class 1 actives.

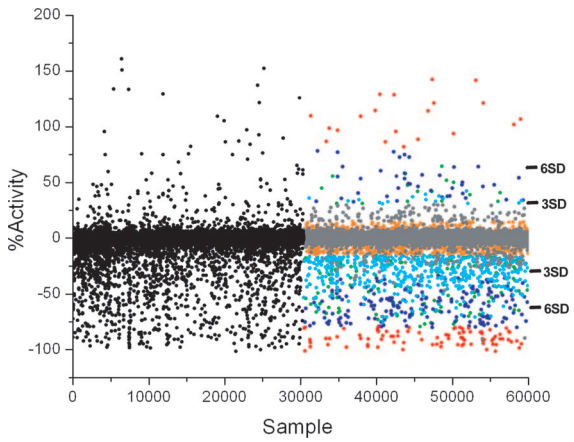

Fig. 5. Analysis of single-concentration screening data at 11 μM. A scatter plot of the 11 μM data, with the right half colored by the curve class as follows: Class 1a (red), Class 1b (green), Class 2a (dark blue), Class 2b (light blue), Class 3 (orange), and Class 4 inactives (gray). The thresholds for three and six SD are indicated. Analysis based exclusively on a three and six SD activity selection threshold (i.e., without the aid of curve classification, left side of the figure) results in confirmed positives, false positives, and false negatives of 1,431 (98%), 30 (2%), and 845 (40%), 534 (99%), 5 (1%), and 1,602 (75%), respectively.

Whereas false positives can be detected with follow-up testing, false negatives cannot be identified by traditional HTS, and, hence, little is known about their frequency. Using our retrospective analysis, we looked for compounds that showed Class 1 and 2 curves that did not score as positive when the 11 μM data set and a three- or six-SD threshold were used. Class 3 curves were not included because they represented activities at only the highest concentration. Above three SD, 845 (40%) compounds were not identified. Because these compounds were associated with concentration–response curves, they were false negatives. Above the six-SD threshold, the number of false negatives increased to 1,602, or 75% of the Class 1 and 2 curves (Fig. 5). These numbers of false negatives were quite high, especially in light of the excellent performance of the assay and low false positives (≤2%). These results indicate that single-concentration screening followed by analysis using thresholds and scatter plots does not score compound activity dependably (Fig. 5).

Derivation of SAR. qHTS fully characterizes the potency and efficacy of the entire library, enabling derivation of SAR directly from the primary screen. To identify active scaffolds, compounds associated with Class 1a, 1b, and 2a curves were used for hierarchical clustering using Leadscope (Columbus, OH) fingerprints to yield a primary data set of 55 clusters. Maximal common substructures (MCSs) were extracted from each cluster and then used to search the entire screening collection to find all analogs, including inactives. This process provided a comprehensive set of SAR series with a high degree of confidence, because the extraction of MCSs was based on compounds having complete titration curves that were subsequently used to find weak and inactive analogs. Each series can be further refined by using other functions such as potency, Hill slope, or efficacy to provide biological context.

An SAR analysis yielded 40 series composed of 4–25 active analogs. Four series are shown in Fig. 6. The first cluster, a flavonoid scaffold, contained 56 analogs of 0.19–89 μM potency as well as 20 inactive compounds (Fig. 6*a*). This family of natural products is known to interact with protein kinases such as Src (15). Series 2, an imidazo thiazole scaffold, contained four analogs, including the most potent (55 nM) compound identified in the screen (Fig. 6*b*). Series 3, a quinazoline scaffold from a 1,000-member combinatorial library, contained 83 analogs of low potency, indicating that this series is refractory to improvements of potency (Fig. 6*c*). Series 4, a *tert*-butyl pyrazolo pyrimidinone scaffold, was composed of eight active analogs, including both an inhibitor and an activator associated with Class 1 curves (Fig. 6*d*). *R* group analysis showed that benzyl substitutions were stimulatory, whereas benzyl ester and

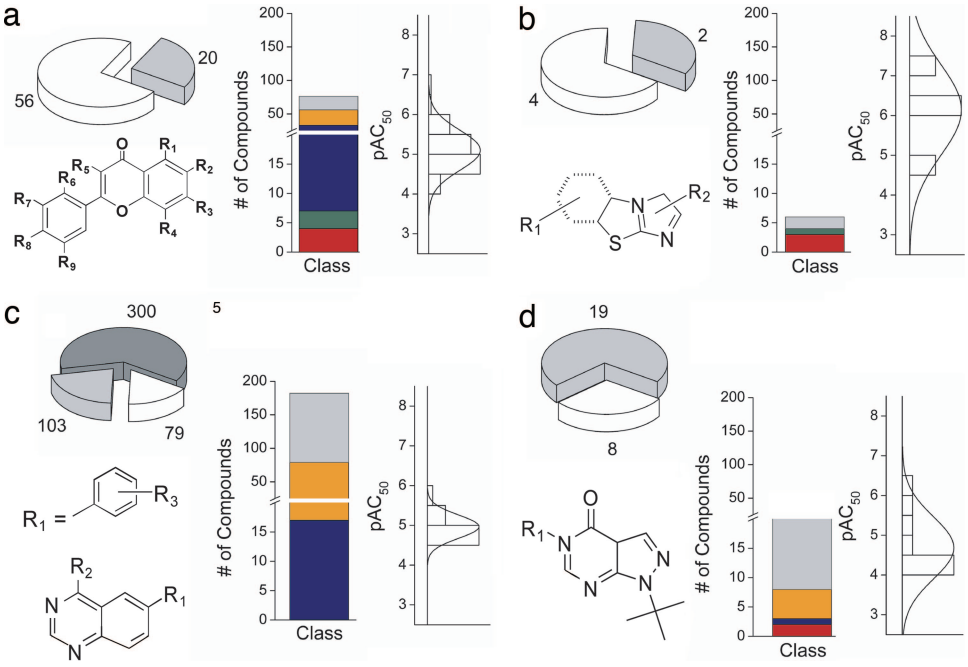

Fig. 6. Pharmacological profile of four analog series. (*a–d*) Potency and curve class distribution of four representative scaffolds. Curves corresponding to Class 1a (red), Class 1b (green), Class 2 (blue), Class 3 (orange), and inactive (gray) are depicted in the bar charts. Curve Classes 1–3 (white) and Class 4 (light gray) are indicated in the pie charts. (*c*) Additional inactives containing a quinazoline core but lacking a phenyl substituent at position R1 (dark gray) are shown in the pie chart. Normal distribution was calculated as described in Fig. 4.

benzyl amide substitutions were inhibitory (Fig. 9, which is published as supporting information on the PNAS web site).

Discussion

The qHTS method presented here addresses many of the fundamental issues of data quality that are required for a reliable and useful public database of compounds and associated biological activities. This approach eliminated false positives and false negatives common to traditional HTS, was highly reproducible, and yielded comprehensive SAR.

Underpinning qHTS is the use of interplate titrations and assay miniaturization. Interplate titrations allow customization of the screening concentrations depending on the availability of reagents or assay design. For example, an equilibrium binding assay between weakly interacting components present at micromolar concentrations limits the AC_{50} to the micromolar range, obviating compound titrations below this level. Whereas we chose a minimum of seven 5-fold dilutions for the titration series to cover a broad concentration range, any number, dilution, or variation can be used. For instance, asymmetric titrations targeting more points per decade at higher concentrations than the lower ones may improve the confidence in curve fit for lower-potency compounds (e.g., Class 2 and 3). However, the minimum number of titration points depends on the nature and variability of the assay. Whereas reliable AC_{50} determinations from two points (1 and 10 μM) have been demonstrated by using constrained fitting (slope and upper and lower asymptotes held constant), seven points produce reliable unconstrained concentration–response curves when modeled for a range of response error (16, 17). Additionally, because each titration series is screened from low to high concentration, carryover of active compounds is easily identified because they appear as reverse titrations. Furthermore, the distributed nature of interplate titrations reduces the effect of failures that may affect a plate within a series; if a single plate is lost, activity curves can still be generated from the remaining plates of the titration. Finally, all compound concentrations are assayed at the same well position in the plate series, which minimizes the variations caused by positional effects.

Miniaturization is required for the efficiency and cost-effectiveness of titration-based screening. For example, a qHTS using a seven-point titration series in 1,536-well plate format results in only 1.75-fold additional plates handled compared with a screen at single concentration in 384-well format. The reagent volumes consumed are unchanged, whereas compound use is reduced.[†] This additional plate handling is compensated by eliminating the need to cherry pick and retest compounds in separate experiments, thereby conserving time and compound.

qHTS shifts the analysis of screening data from a statistical to a pharmacological process. This method prevents assigning compounds as active or inactive based on stochastic variation, a common occurrence with traditional HTS and a major factor necessitating the cherry-picking process. Compounds having partial activity or low efficacy can represent important modulators of biological activity and are particularly difficult to recognize via traditional HTS, but easily identifiable with qHTS. For example, in a recent cellular assay to identify stabilizers of IκBα, we observed a potent (20 nM) but partial (25% of control activity) effect of hydrocortisone that reproduced accurately upon retesting (D.S.A., unpublished results). Additionally, a compound's potency and efficacy often depends on assay design. For example, choice of cell type and endpoint can affect the apparent potency of a compound, in some cases leading to a significant rightward shift in AC_{50} (2, 18, 19). In single-concentration screening, the identification of a compound depends highly on assay design. In contrast, qHTS is resilient to variations in assay sensitivity.

Using qHTS, we retrospectively enumerated the false-positive and -negative burden from a single-concentration screen (see Fig. 5; and see Table 2, which is published as supporting information on the PNAS web site). Two percent of the actives scored as false positives, and 40% of the Class 1 to 2 actives were false negatives when the 11 μM screening concentration[‡] and a three SD threshold (Fig. 5) were used. The high precision of the PK assay ($Z' = 0.87$) resulted, in large part, from a luminescence signal and large signal/background ratio. Assays with higher intrinsic variability, such as those using cell-based reporter or phenotypic outputs, are expected to have greater assignment error, with false positives

[†]Calculations are based on 30- and 4-μl well volumes for 384- and 1,536-well plates, respectively.

[‡]Additional analysis comparing qHTS with the maximal concentrations screened is given in supporting information.

as high as 90% (20). We are now using qHTS to analyze cell-based assays to quantitate the extent of false positives and false negatives.

Traditional HTS limits the accurate assessment of a compound's activity because the screens are conducted at micromolar concentrations, whereas the AC_{50} values for small molecules range broadly from picomolar to millimolar. Given this range in compound potency represented in large compound libraries, screening at a single concentration necessarily tests some compounds at well below their AC_{50} where no effect is detected and others at well above their AC_{50} where cellular toxicity or other adventitious effects are observed. For instance, flavonoids have been identified as promiscuous inhibitors at 10 μM (21); however, in our qHTS study, we found a series of flavonoids that selectively inhibited PK or luciferase (PubChem Assay ID 361 and 411), indicating a pharmacological basis for their activity.

Highly focused libraries, such as those derived from combinatorial chemistry (CC) are particularly confounding when screened at a single concentration point, because they contain large numbers of highly related structural analogs, resulting in a "leveling effect," where many compounds are scored as active, but their relative activity is obscured, thereby limiting the usefulness of CC libraries. In contrast, qHTS can distinguish the potencies and efficacies of closely related analogs in CC libraries. We have observed such a series from a qHTS of cytochrome P450 1A2, where a quinazoline scaffold containing 98 analogs displayed a potency range of 32 nM to 10 μM, indicating broad SAR over a narrow structural field (PubChem Assay ID 410).

The primary goal of HTS development to date has been to increase screening throughput. However, despite the many new statistical methods developed to analyze the data (22), this focus on throughput has lead to the generation of large but frequently uninformative data sets because of the persistence of false positives, false negatives, or ineffective screening concentrations. Experimentally, the use of replicates in single-concentration screening has been implemented in some cases to increase the confidence of selecting biologically active compounds. However, limitations remain, because the relationship of replicates is solely statistical not pharmacological, as the dose is not varied. By changing the experimental design to titration-based screening, an overreliance on the statistical treatment of noisy data is alleviated. Broad adoption of this paradigm should move HTS into the realm of high-throughput pharmacology, providing robust databases of structure–activity relationships suitable for both improving the early phase drug discovery process and enabling the longer-term establishment of a chemical genomic database.

Materials and Methods

Preparation of Compound Titration Plates. The 60,793-member library was prepared as DMSO solutions at compound concentrations ranging between 2 and 10 mM. Plate-to-plate dilutions were performed in 384-well plates by using an Evolution P^3 system (PerkinElmer, Wellesley, MA) equipped with a 384-well head. Compression of 384-well plates to 1,536-well plates was also performed by using the Evolution P^3 system.

PK qHTS. Three microliters per well of buffered substrate was added to 1,536-well plates by using a solenoid-based dispenser. Compound was transferred to the assay plates by using a 23-nl 1,536-pin array. After transfer, 1 μl per well of enzyme mix was added. The plates were centrifuged at 157 $\times$ *g* for 30 s and incubated for 2 h at ambient temperature, followed by addition of 3 μl per well of detection and kinase stop solution. After a 10-min incubation, luminescence was detected by a CCD-based plate reader. All screening operations were performed by using a fully integrated robotic system (Kalypsys, San Diego, CA) containing one RX-130 and two RX-90 anthropomorphic robotic arms (Staübli, Duncan, SC).

Data Analysis. Screening data were corrected and normalized and concentration–effect relationships derived by using the GeneData Screener software package. Concentration–effect relationships were categorized according to fit quality (r^2), response magnitude, and degree of measured activity. Active compounds were clustered according to structural similarity and curve classifications by using Leadscope software. Complete SARs were determined by using all members structurally related to active core scaffolds.

Supporting Text. For details on the preparation of the compound titration plates, PK qHTS, and data analysis, see *Supporting Text*, which is published as supporting information on the PNAS web site.

We thank S. Michael and C. Klumpp for assistance with the automated screening. This work was supported by the Molecular Libraries Initiative of the National Institutes of Health Roadmap for Medical Research and the Intramural Research Program of the National Human Genome Research Institute, National Institutes of Health.

1. Hill, A. V. (1910) *J. Physiol. (London)* **40,** 4–7.
2. Kenakin, T. (2003) *Nat. Rev. Drug Discov.* **2,** 429–438.
3. Hardman, J. G., Limbird, L. E. & Gilman, A. G. (2001) *Goodman & Gilman's The Pharmacological Basis of Therapeutics* (McGraw–Hill, New York).
4. Schnecke, V. & Bostrom, J. (2006) *Drug Discov. Today* **11,** 43–50.
5. Malo, N., Hanley, J. A., Cerquozzi, S., Pelletier, J. & Nadon, R. (2006) *Nat. Biotechnol.* **24,** 167–175.
6. Austin, C. P., Brady, L. S., Insel, T. R. & Collins, F. S. (2004) *Science* **306,** 1138–1139.
7. The PubChem Project, National Center for Biotechnology Information. http://pubchem.ncbi.nlm.nih.gov.
8. Sakai, H., Suzuki, K. & Imahori, K. (1986) *J. Biochem. (Tokyo)* **99,** 1157–1167.
9. Munoz, M. E. & Ponce, E. (2003) *Comp. Biochem. Physiol. B* **135,** 197–218.
10. Zhang, J. H., Chung, T. D. & Oldenburg, K. R. (1999) *J. Biomol. Screen.* **4,** 67–73.
11. Eastwood, B. J., Farmen, M. W., Iversen, P. W., Craft, T. J., Smallwood, J. K., Garbison, K. E., Delapp, N. W. & Smith, G. F. (2006) *J. Biomol. Screen* **11,** 253–261.
12. Popa-Burke, I. G., Issakova, O., Arroway, J. D., Bernasconi, P., Chen, M., Coudurier, L., Galasinski, S., Jadhav, A. P., Janzen, W. P., Lagasca, D., *et al.* (2004) *Anal. Chem.* **76,** 7278–7287.
13. Segel, I. H. (1975) *Enzyme Kinetics: Behavior and Analysis of Rapid Equilibrium and Steady-State Enzyme Systems* (Wiley, New York), pp. 188–190.
14. Buxser, S. & Vroegop, S. (2005) *Anal. Biochem.* **340,** 1–13.
15. Sicheri, F., Moarefi, I. & Kuriyan, J. (1997) *Nature* **385,** 602–609.
16. Morelock, M. M., Hunter, E. A., Moran, T. J., Heynen, S., Laris, C., Thieleking, M., Akong, M., Mikic, I., Callaway, S., DeLeon, R. P., *et al.* (2005) *Assay Drug Dev. Technol.* **3,** 483–499.
17. Turner, R. J. & Charlton, S. J. (2005) *Assay Drug Dev. Technol.* **3,** 525–531.
18. Berg, K. A., Maayani, S., Goldfarb, J., Scaramellini, C., Leff, P. & Clarke, W. P. (1998) *Mol. Pharmacol.* **54,** 94–104.
19. Christopoulos, A., Christopoulos, G., Morfis, M., Udawela, M., Laburthe, M., Couvineau, A., Kuwasako, K., Tilakaratne, N. & Sexton, P. M. (2003) *J. Biol. Chem.* **278,** 3293–3297.
20. Gribbon, P., Lyons, R., Laflin, P., Bradley, J., Chambers, C., Williams, B. S., Keighley, W. & Sewing, A. (2005) *J. Biomol. Screen.* **10,** 99–107.
21. Feng, B. Y., Shelat, A., Doman, T. N., Guy, R. K. & Shoichet, B. K. (2005) *Nat. Chem. Biol.* **1,** 146–148.
22. Glick, M., Jenkins, J. L., Nettles, J. H., Hitchings, H. & Davies, J. W. (2006) *J. Chem. Inf. Model* **46,** 193–200.